Available online at www.sciencedirect.com
SCIENCE DIRECT®
Journal of Power Sources 119–121 (2003) 460–464
JOURNAL OF POWER SOURCES
www.elsevier.com/locate/jpowsour

Charge–discharge studies on a lithium cell composed of PVdF-HFP polymer membranes prepared by phase inversion technique with a nanocomposite cathode

A. Manuel Stephan[1], Dale Teeters[*]

Department of Chemistry and Biochemistry, The University of Tulsa, 600 S. College Avenue, Tulsa, OK 74104-3189, USA

Abstract

A novel polymer membrane of poly(vinylidene fluoride-hexafluoropropylene) (PVdF-HFP) co-polymer was prepared by the phase inversion technique with two different non-solvents, 1-butanol or hexane. The prepared films were analyzed by scanning electron microscope (SEM) and nitrogen absorption/desorption techniques. The change in the morphology and pore diameter of the films prepared with different non-solvents correlates with the structure of the non-solvents used. This electrolyte membrane was coupled with a nanocomposite $LiAl_{0.01}Co_{0.99}O_2$ cathode which was prepared by a solid-state reaction method and subsequently by ball-milling. Lithium cells consisting of $LiAl_{0.01}Co_{0.99}O_2$/polymer electrolyte/Li were assembled and their charge–discharge studies were investigated.

Keywords: Phase inversion technique; Pore diameter; Solid-state reaction; Charge–discharge studies; Nanocomposite cathode

1. Introduction

The applications of gel polymer electrolytes in rechargeable lithium batteries are currently being investigated because they have several advantages such as high energy density, freedom from leakage and a flexible geometry [1,2]. Common gel polymer electrolytes exhibit high ionic conductivity; however, their mechanical properties are not sufficient for practical applications [3–5]. The recent attention given to gel polymer electrolytes where a liquid electrolyte is contained in a mesoporous polymer film is thus not only because of high ionic conductivity but also because of good mechanical properties as well [6]. These types of gel polymer electrolytes are prepared by immersing a polymer matrix in a liquid electrolyte. The electrolyte permeates pores in the polymer matrix that resulted from earlier removal of solvent from the polymer film [7]. The conductivity of the electrolyte is dominated by the amount of the liquid electrolyte absorbed by the polymer matrix. Membrane porosity, tortuosity of the pores, the conductivity of the electrolyte, the thickness of the membrane and the extent to which the electrolyte wets the pores of the membrane also play an important role in the development of polymer membranes for battery applications [8].

Recently, microporous poly(vinylidene fluoride-hexafluoropropylene) (PVdF-HFP) membranes were developed by Bellcore in which dibutyl phthalate was used as an additive; however, the conductivity of the films was expectedly low [8]. Enhancement of conductivity was achieved by the addition of fumed silica, but these films unfortunately suffer poor rate capability when they were used as separators in lithium ion cells [9].

When considering the cathode component of the lithium battery, lithium cobalt oxide is the most widely used material in commercially available batteries due to its ease of preparation and high theoretical specific capacity [12]. $LiCoO_2$ materials, however, require some modifications to improve electrode performance, such as substitution of Co with other metal ions in order to stabilize the layered structure [13]. Being a lighter and less expensive metal than cobalt, Al-doped $LiCoO_2$ has several advantages such as higher intercalation voltage, higher energy density and lower cost [14]. Al-doped $LiCoO_2$ also has thermal stability and decreased heat of reaction compared to pure $LiCoO_2$ cathodes.

Recently, the importance and preparation of nanoscale cathode materials, for instance by ball-milling, for applications in lithium secondary batteries have been well demonstrated by Goodenough and co-workers [15], Wang et al. [16], and also by us [17,18]. Manev et al. [19] have proved

* Corresponding author. Tel.: +1-918-631-3147; fax: +1-918-631-3404.
E-mail address: dale-teeters@utulsa.edu (D. Teeters).
[1] Present address: Advanced Battery Division, Central Electrochemical Research Institute, Karaikudi 630 006, India.

0378-7753/03/$ – see front matter © 2003 Published by Elsevier Science B.V.
doi:10.1016/S0378-7753(03)00198-8

that smaller particles are more flexible than larger particles during cycling and the changes in the lattice parameters are only slightly affected. In the present work, we used solid-state reaction methods to synthesis $LiAl_{0.01}Co_{0.99}O_2$ and employed ball-milling to get particles on the nanoscale. To the best of our knowledge, very little research has been carried out on the preparation of nanoparticles of $LiCoO_2$ and its charge–discharge behavior.

In the present study, an attempt has been made to explore how the non-solvents affect membrane morphology, and how the change in pore-size distribution of the membranes affect the charge–discharge properties when they are used as separators in lithium ion cells. Another area of investigation was the compatibility of the Al-doped nanoparticle $LiCoO_2$ with the nanopore polymer membranes during battery cycling.

2. Experimental

2.1. Polymer membranes

Microporous polymer films were obtained by the phase inversion technique as described elsewhere [7–11]. PVdF-HFP co-polymer (Elf Atochem, Japan) was dissolved in a solvent with a volume ratio of 1:3, respectively, of acetone (the volatile solvent) and hexane or 1-butanol (the non-solvents). The amount of the non-solvent was low enough to allow initial solublization, but also high enough to allow phase separation upon evaporation of the acetone.

The resulting solution was spread as a film on a glass substrate and the solvents were allowed to evaporate at ambient temperature. Any remaining non-solvents were removed by vacuum drying for 12 h at 110 °C. All experiments were performed in a dry room. Morphological examination of the films was made using a JSM-5410LV scanning electron microscope (SEM) under vacuum (10^{-1} Pa) after sputtering gold on one side of the films. The BET surface area and pore-size distribution were determined by a continuous-flow nitrogen gas apparatus (BELSORP 28, Japan).

2.2. Cathode

$LiAl_{0.01}Co_{0.99}O_2$ powders were synthesized by solid-state reaction methods. A stoichiometric amount of Li_2CO_3, Co_3O_4 and $Al(OH)_3$ were ground and calcined at 400 °C for 12 h and then at 800 °C for 24 h with intermittent grinding. The crystal structure of $LiAl_{0.01}Co_{0.99}O_2$ calcined at 800 °C was characterized by XRD. The prepared cathode material was ball-milled for 2 h to get particles that were on the nanoscale.

2.3. Cells

The cathode was prepared by brush-coating a slurry of 85% $LiAl_{0.01}Co_{0.99}O_2$, 5% poly(vinyledene fluoride) and 10% acetylene black in 1-methyl-2-pyrrolidinone on an aluminum substrate and then drying in a vacuum oven at 120 °C for 12 h. The prepared polymer membrane was soaked in the electrolyte solution composed of $LiPF_6$ dissolved in a solvent of ethylene carbonate and dimethyl carbonate having a volume ratio of 2:1. Lithium foil was used as the anode. The $LiAl_{0.01}Co_{0.99}O_2$/polymer electrolyte/Li cells were assembled in an argon filled glove box.

3. Results and discussion

The SEM pictures (Figs. 1 and 2) reveal the morphology of the polymer membranes prepared with hexane and 1-butanol, respectively. A more homogenous phase with uniformly sized pores was achieved when the linear aliphatic non-solvent, hexane, was used. In contrast, a flaky surface with unevenly sized pores developed when 1-butanol was used as the non-solvent.

As shown in Fig. 3, almost all pores of PVdF-HFP membranes prepared with hexane and 1-butanol are, according to IUPAC convention, ‘‘mesopores’’ i.e. pores with diameters ranging from 2 to 50 nm. The mean pore diameter and BET surface area of Celgard 2400, determined by a

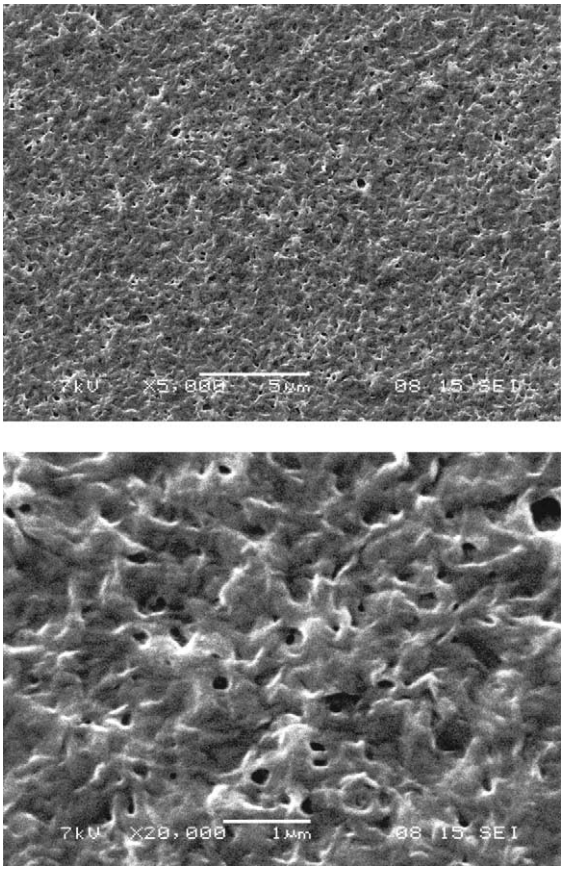

Fig. 1. SEM images of PVdF-HFP membrane prepared with hexane as the non-solvent.

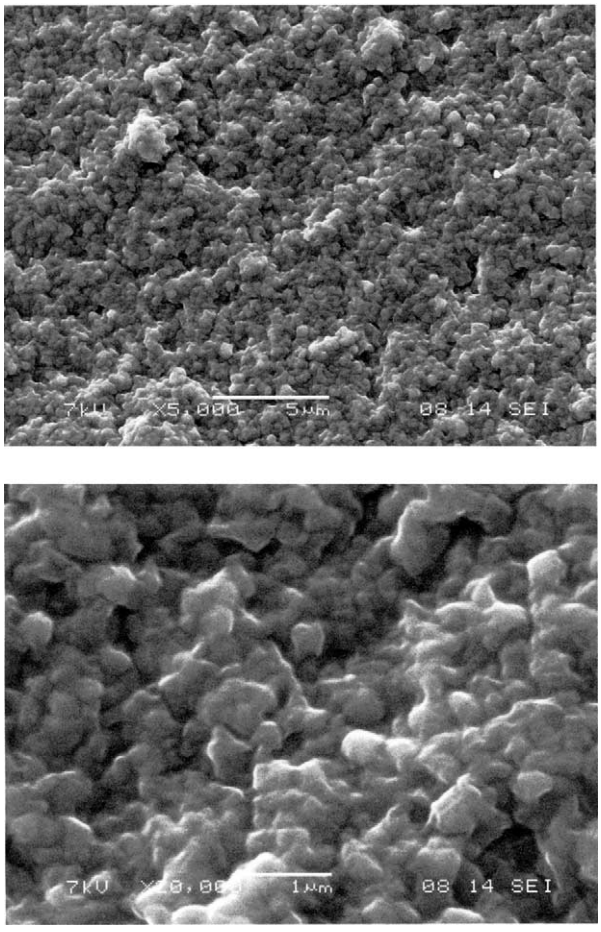

Fig. 2. SEM images of PVdF-HFP membranes prepared with 1-butanol as the non-solvent.

continuous-flow nitrogen gas adsorption apparatus similar to the one used in this study, are 36 nm and 41.76 $m^2\ g^{-1}$, respectively [7]. In comparison, the films prepared with hexane and 1-butanol as the non-solvents have pore diameters and BET surface areas of 4 nm and 218 $m^2\ g^{-1}$, and 10 nm and 40.76 $m^2\ g^{-1}$, respectively. Large porosities and smaller pore diameters are two prerequisites of good separators for rechargeable lithium batteries. Assuming that a smaller pore diameter is desirable, the PVdF-HFP prepared by the phase inversion technique, with hexane as the non-solvent, seems to be better than Celgard 2400. However, in terms of pore diameter, the films prepared with 1-butanol are similar to Celgard 2400 separators.

These results indicate that the morphology of the phase-separated membrane may be tailored by the nature of the non-solvent used. The smaller pore diameters of the films obtained with hexane may be attributed to several factors. First, the linearity of the hexane molecules may result in an escape path with a small diameter through the polymer matrix during the slow evaporation of the non-solvent. Also, these aliphatic, non-polar, hydrocarbon molecules should minimize interaction with any of the hetero-atoms in the PVdF-HFP co-polymer chain. On the other hand, the 1-butanol molecule would have more attractions to the co-polymer chain, making its escape route to the surface more tenuous thus resulting in larger pores.

Fig. 4 shows the XRD of the $LiAl_{0.01}Co_{0.99}O_2$ sample calcined at various temperatures for 24 h in air. This sample was first "precalcined" at 200 °C for 6 h and then calcined 800 °C for 18 h. The XRD for this solid-state derived $LiAl_{0.01}Co_{0.99}O_2$ powder, calcinated at 800 °C, shows good separation of diffraction lines, which indicates that these materials are well-layered structures. The widths of the peaks are narrow, indicating an increase in crystallinity of the material.

Fig. 5a shows the XRD patterns of $LiAl_{0.01}Co_{0.99}O_2$ and Fig. 5b shows the XRD patterns of $LiAl_{0.01}Co_{0.99}O_2$ ball-milled for 2 h. From the XRD peaks of ball-milled $LiAl_{0.01}Co_{0.99}O_2$, we observe a decrease in intensity as well as broadening of the peaks. The TEM image of the ball-milled $LiAl_{0.01}Co_{0.99}O_2$ shown in Fig. 6 and the broadening of the

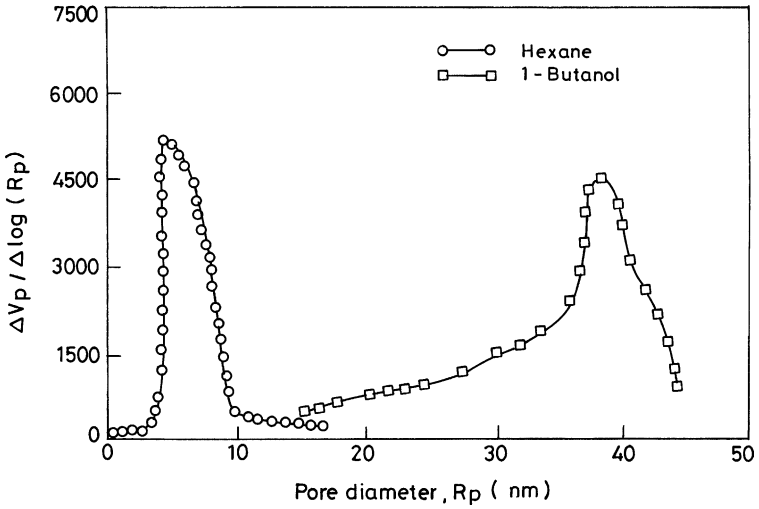

Fig. 3. Pore-size distribution for membranes prepared with hexane (○) and 1-butanol (□) as the non-solvents.

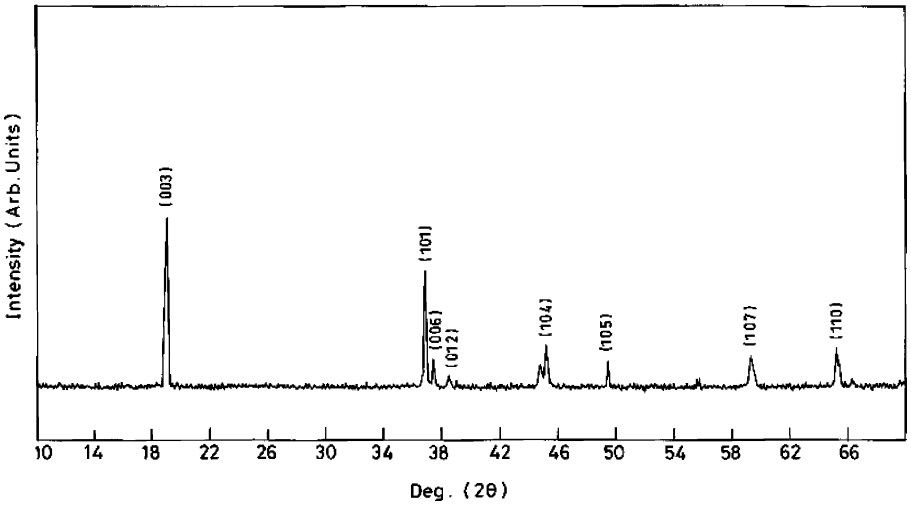

Fig. 4. XRD of $LiAl_{0.01}Co_{0.99}O_2$ calcined at 800 °C.

XRD peaks in Fig. 5, similar to that seen by Kang et al. for similar systems [15], show that the material was broken into nanoparticles. In addition, many nanograins were generated within a large crystalline matrix by the action of defects. The TEM image shows a substantial particle agglomeration most likely due to a high degree of crystallization at high temperature. However, the average particle size of the $LiAl_{0.01}Co_{0.99}O_2$ within the agglomerates can still be seen to be 50–100 nm.

Fig. 7 shows the variation of discharge capacities during cycling between 2.7 and 4.3 V at *C*/10 rate for $LiAl_{0.01}Co_{0.99}O_2$ samples calcined at 800 °C and also for $LiAl_{0.01}Co_{0.99}O_2$ samples ball-milled for 2 h coupled with the hexane and the 1-butanol prepared PVdF-HFP polymer films. The difference in structure and pore-size between the two PVdF-HFP films seems to have only small effects on the cell performance. However, the $LiAl_{0.01}Co_{0.99}O_2$ cells without ball-milling exhibit a lower initial capacity and also suffer large capacity fading. After 15 cycles, the discharge capacity for these systems decreased below 45% of the initial capacity. These results are in accordance with those reported earlier [20]. However, the capacity fading of the ball-milled

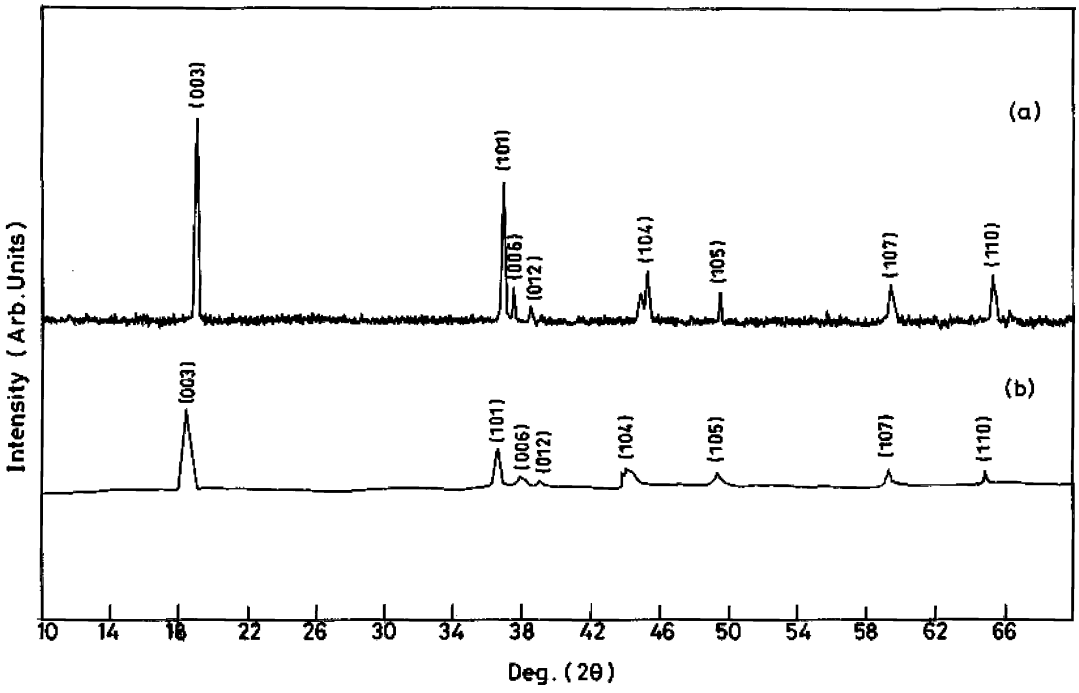

Fig. 5. XRD of $LiAl_{0.01}Co_{0.99}O_2$: (a) without ball-milling, and (b) after ball-milling for 2 h.

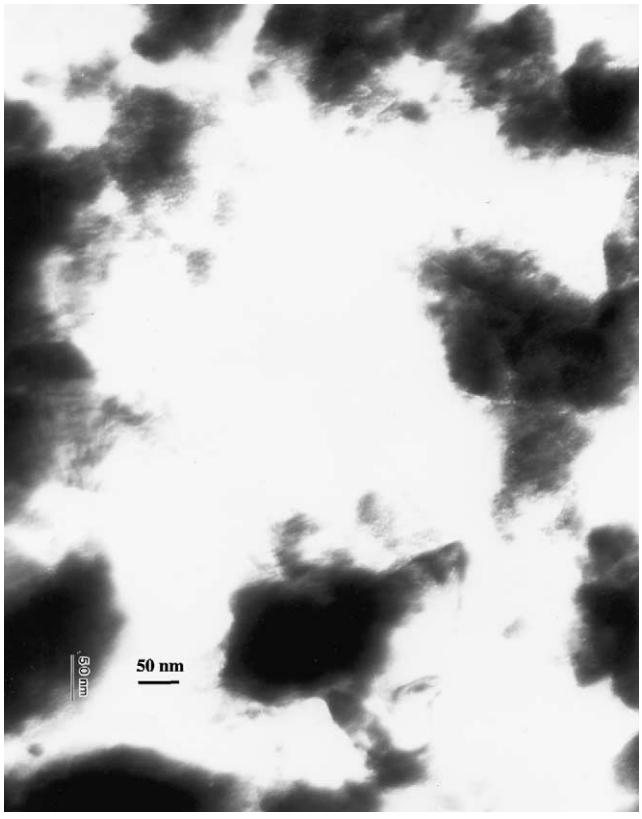

Fig. 6. TEM image of $LiAl_{0.01}Co_{0.99}O_2$ ball-milled for 2 h.

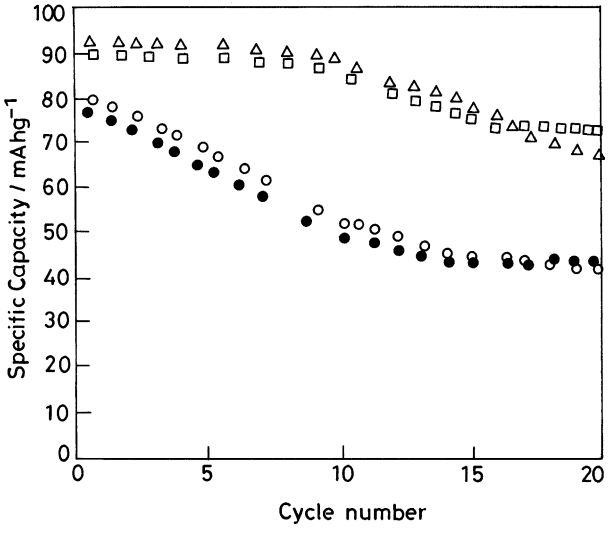

Fig. 7. Cycling performance of $LiAl_{0.01}Co_{0.99}O_2$ cells with PVdF-HFP membranes. Without cathode ball-milling: with hexane (○) and 1-butanol (●) as the non-solvents. With cathode ball-milling: with hexane (△) and 1-butanol (□) as the non-solvents.

$LiAl_{0.01}Co_{0.99}O_2$ samples was greatly decreased, apparently due to the decrease in particle size of the cathode materials. This can be attributed to the increase of lithium ion conductivity through the nanoparticles of the cathode [15].

4. Conclusions

The PVdF-HFP co-polymer membrane, prepared by the phase inversion methods with hexane as a non-solvent, exhibited smaller pore diameters and a higher BET surface area than those prepared with 1-butanol. Although the morphology and pore diameters were different for the two non-solvents used, only small changes in the charge–discharge characteristics could be attributed to the film differences. On the other hand, the incorporation of nanoparticles in the cathode improves charge–discharge properties. This nanoparticle composite cathode also appears suitable for use with the nanoporous membrane separators described here.

Acknowledgements

The authors would like to than the Office of Naval Research for funding this research through grant N00014-01-1-0724.

References

[1] D.W. Kim, J.M. Ko, J.H. Chun, J. Power Sources 93 (2001) 151.
[2] B. Scrosati, Applications of Electroactive Polymers, Chapman & Hall, London, 1993.
[3] A. Manuel Stephan, N.G. Renganathan, S. Pitchumani, N. Muniyandi, J. Power Sources 81–82 (1999) 752.
[4] A. Manuel Stephan, N.G. Renganathan, S. Pitchumani, N. Muniyandi, J. Power Sources 83 (2000) 80.
[5] A. Manuel Stephan, N.G. Renganathan, S. Pitchumani, N. Muniyandi, Solid State Ionics 130 (2001) 123.
[6] A.S. Gozdz, C.W. Schmutz, J.M. Tarascon, P.C. Warren, US Patent 5,540,741 (1997).
[7] J.Y. Song, Y.Y. Wang, C.C. Wan, J. Electrochem. Soc. 147 (2000) 3219.
[8] H. Wang, H. Huang, S.L. Wunder, J. Electrochem. Soc. 147 (2000) 2853.
[9] Y. Saito, H. Kataoka, A. Manuel Stephan, Macromolecules 34 (2001) 6955.
[10] A. Manuel Stephan, H. Kataoka, Y. Saito, Solid State Ionics, in press.
[11] A. Manuel Stephan, Y. Saito, Solid State Ionics 148 (2002) 475.
[12] K. Ozawa, Solid State Ionics 69 (1994) 212.
[13] R. Alcantara, P. Larcla, P.L. Relando, J.L. Tirado, E. Zhechera, R. Stoyanora, Inorg. Chem. 37 (1998) 264.
[14] G. Ceder, Y.M. Chiang, D.R. Sadoway, M.K. Aydinol, Y.I. Jang, B. Huang, Nature 392 (1998) 694.
[15] S.H. Kang, J.B. Goodenough, L.K. Rabenberg, Electrochem. Solid State Lett. 4 (5) (2001) A49.
[16] C.S. Wang, G.T. Wu, W.Z. Li, J. Power Sources 76 (1998) 1.
[17] A. Manuel Stephan, D. Teeters, Electrochim. Acta, in press.
[18] A. Manuel Stephan, D. Teeters, J. Power Sources, submitted for publication.
[19] V. Manev, W. Ebner, W. Thompson, S. Dow, US Patent 5,961,949 (1999).
[20] Y.I. Jang, B. Hung, H. Wang, D.R. Sadoway, G. Ceder, Y.M. Chiang, X. Li, H. Tamura, J. Electrochem. Soc. 146 (1999) 862.